Study of solar parameters causing major geomagnetic storms during SC 23

C. Oprea[1], M. Mierla[1,2,4], D. Besliu-Ionescu[1,3], O. Stere [1], G. Maris Muntean[1]

1 Institute of Geodynamics of the Romanian Academy, Bucharest, Romania
2 STCE - Royal Observatory of Belgium, Brussels, Belgium
3 MoCA, School of Mathematical Sciences, Monash University, Clayton, Victoria, Australia
4 Research Center for Atomic Physics and Astrophysics, Faculty of Physics, University of Bucharest, Romania

Outline:

Data description

Data analysis

- *CME-Flare dependence*
- *CME speeds analysis*
- *Analysis of in-situ parameters and Dst index*
- *Correlation coefficient analysis*
- *Superposed epoch analysis*

Summary

Data Description

SOHO, ACE and different geomagnetic

25 geomagnetic storms with minimum Dst ≤ –150nT occurred in the period between 1998 – 2005

Catalog:

Among CMEs signatures:

- the projected speeds and the heights at which was measured;
- source type and location on the solar disk.

Among ICME signatures:

- beginning and end time of ICME;
- Bz, B, speed, density, temperature.

Solar signatures

- **57 CMEs** directed towards the Earth associated with the 25 major geomagnetic storms
- Full or partial halo CMEs
- Have their origins in complex active regions ($\beta\gamma$ or $\beta\gamma\delta$ magnetic configuration).
- Associated flares with large energy range, from C2.0 to X17.2 class flares;
- Seven events out of 57 have no flare association;
- 14 events were associated with erupting or disappearing filaments.

In-situ signatures

Interplanetary phenomena causing strong geomagnetic storms (Echer et al., 2008):

- Magnetic cloud (MC)
- Magnetic cloud with shock (sMC)
- Magnetic cloud without shock (nsMC)
- Sheath region between the interplanetary shock and MC (Sh)
- Sheath region and MC (Sh+MC)
- Corotating interaction region (CIR)
- Complex structure (Complex)

Geomagnetic signatures

- 25 major geomagnetic storms with clear CMEs associated.
- The minimum Dst index varies from -422 nT to -159 nT.
- Most of the storms have started with a sudden commencement;
- Only two of them presenting at their beginning a gradual commencement
- Three storms had uncertain commencement.

(source: http://www.spacescience.ro/new1/GS HSS Catalogue.htm)

Data Analysis

CME-Flare dependence

The 25 ICMEs in our study are correlated to 57 eruptive events, from which 50 are associated with X-ray flares.

$$Q_x = i_x \cdot t_x$$

i_x - the intensity scale of the importance of X−ray flare spectral class
t_x - the duration of the flare in minutes.
(Maris et al., 2002)

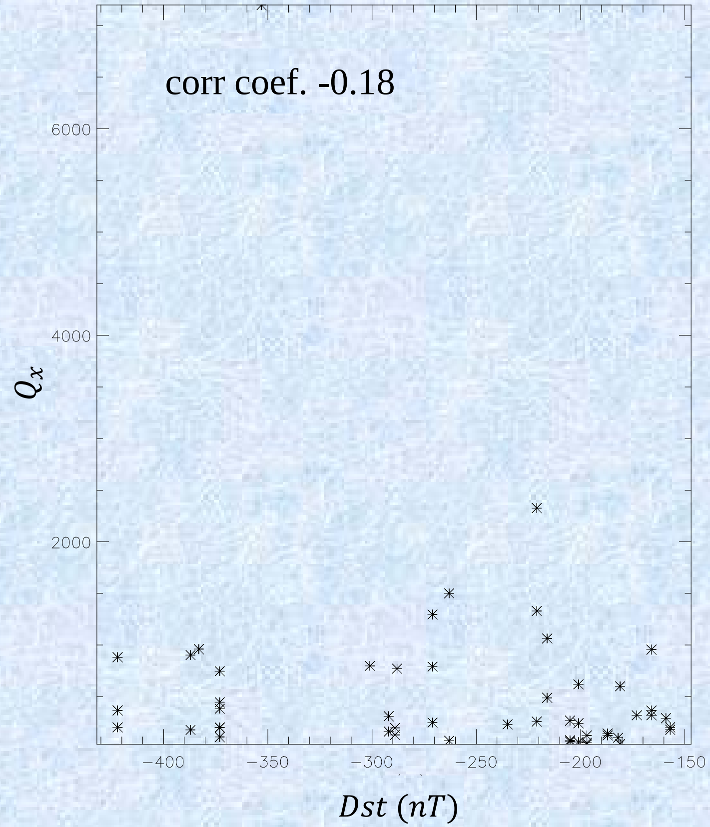

Importance soft X-ray flares indices versus Dst indices

No correlation between the flare importance and the Dst index was found

Nevertheless, two CMEs associated with the strongest flares, class X10 (29.10.2003) and class X17.2 (28.10.2003), produced strong geomagnetic storms: Dst of -383 nT and -353 nT, respectively.

CME speeds analysis

CMEs speeds play an important role in producing major geomagnetic storms

- Data used: the projected speeds from LASCO CME catalog
- We derived the true (radial) speed assuming that the CME is a sphere which expands similarly and propagates radially
- We computed the travel time using both radial and projected speeds assuming that the CME keeps a constant speed from the Sun to the Earth

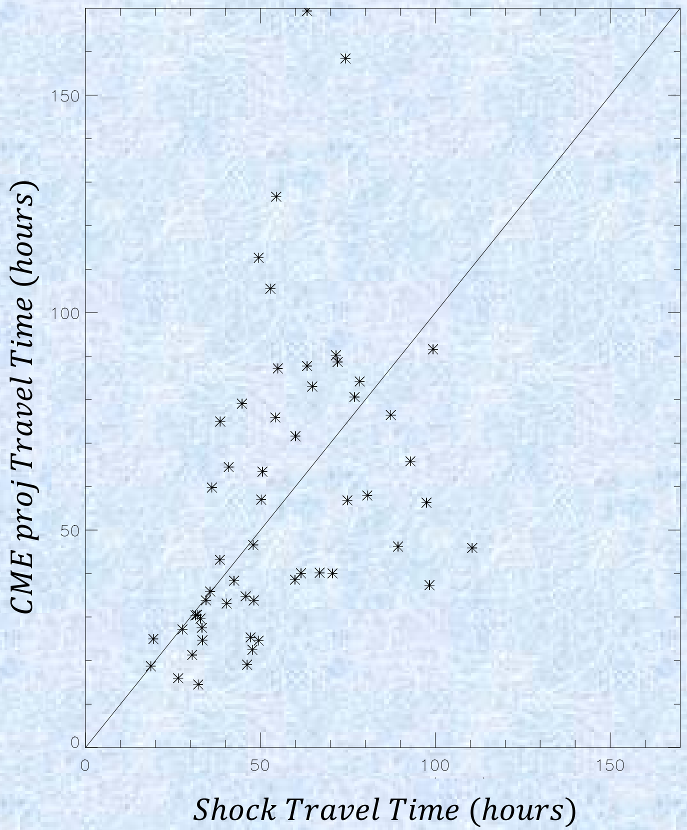

Travel time calculated using the projected speeds versus real travel time

The best correlation with the real travel time was found for the **travel time** calculated using the **projected speeds**

The speed of the CME changed while propagating into the interplanetary space because of the interaction with the ambient solar wind or/and the interaction with other CMEs.

Analysis of in-situ parameters and Dst index

The main three phases of the Solar Cycle 23 :

1. the ascending phase (June 97 – August 99);
2. the maximum phase (September 99 – July 2002);
3. the declining phase (August 2002 – January 2006). (G. Maris, AiP 2010)

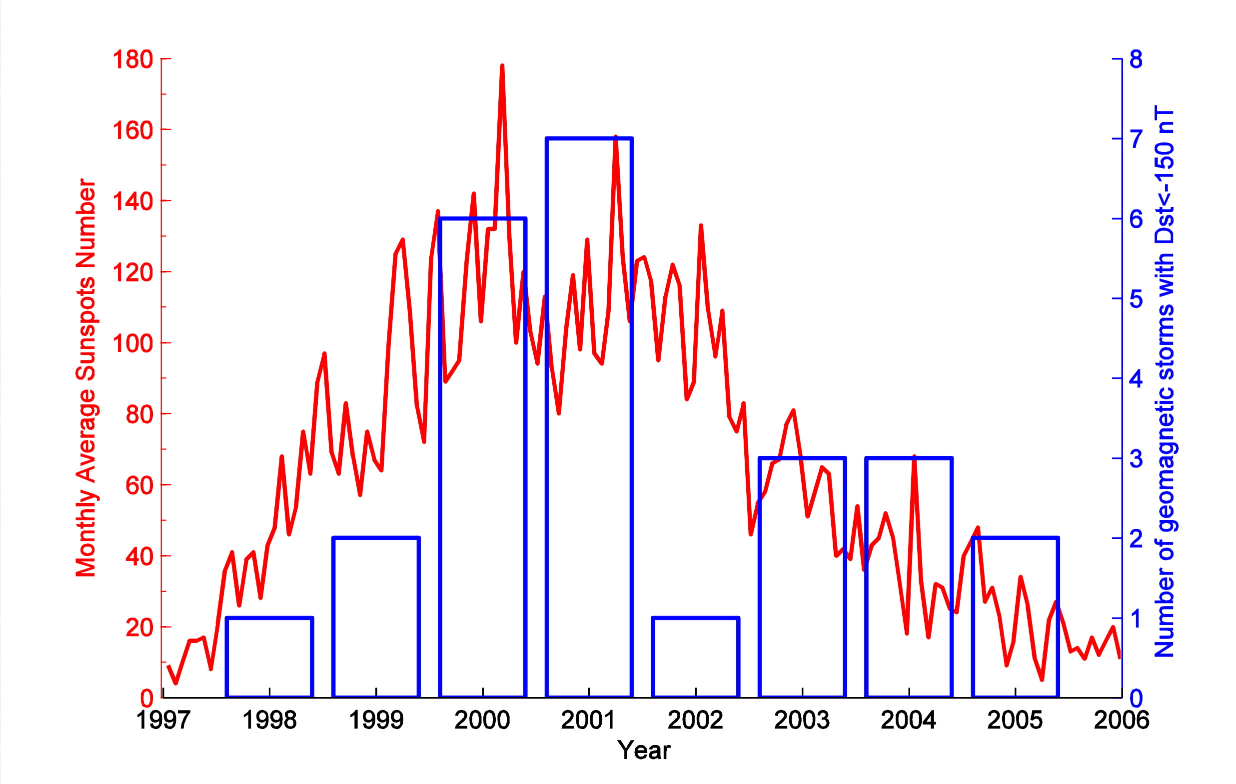

Histogram of the geomagnetic storms with minimum Dst ≤ –150 nT, superposed on the monthly average sunspots number for the SC 23

The distribution of the major geomagnetic storms according to the 23rd SC phases

Minimum Dst (nT)	Ascending Phase (June 97 – August 99)	Maximum Phase (Sept. 99 – July 2002)	Declining Phase (August 2002 – Jan. 2006)
–150 ≥ Dst min > –200	-	7	1
–200 ≥ Dst min > –300	1	7	3
–300 ≥ Dst min > –450	-	2	4

Geoeffectiveness of the interplanetary phenomena on the main three phases for SC 23

	Ascending Phase			Maximum Phase			Declining Phase		
	Dst minimum (nT)			Dst minimum (nT)			Dst minimum (nT)		
Type	-150:-200	-200:-300	-300:-450	-150:-200	-200:-300	-300:-450	-150:-200	-200:-300	-300:-450
MC	-	-	-	-	1	-	-	-	-
sMC	-	-	-	1	-	1	-	2	2
nsMC	-	-	-	1	-	-	-	-	-
Sh	-	1	-	3	2	-	-	-	1
Sh+MC	-	-	-	1	3	1	1	1	1
Complex	-	-	-	1	1	-	-	-	-

- the most geoeffective phenomena in the interplanetary space which caused strong geomagnetic storms are sMC, followed by Sh+MC and the Sh type structures;
- the ICMEs that present magnetic cloud signatures, preceded or not by a shock or a sheath field produced 64% of the total strong geomagnetic storms (Dst ≤ -150nT);
- Sh type structures caused 28% of the total storms;

Correlation coefficient analysis

Correlation coefficients between the Dst geomagnetic index and the ICME parameters

Parameters of IP structures:

- averages of B, plasma speed, proton density and plasma temperature;
- Bz, speed, Bs·V, density, temperature;
- the total energy injected into the magnetosphere in the geomagnetic storms' main phase, W_ε, computed through the Akasofu coupling function (ε).

Bs = |Bz| when Bz < 0 and Bs = 0 when Bz ≥ 0

$$\varepsilon = 10^7 V B^2 l_0^2 sin^4\left(\frac{\theta}{2}\right), \text{[J/s]}$$

where: *V* is the plasma speed, *B* is the IMF, θ is the IMF clock angle in the plane perpendicular to the Sun – Earth line, l_0 is the magnetopause radius, l_0 =7R_E, $\theta = tan^{-1}\left(\frac{B_y}{B_z}\right)$.

$$W_\varepsilon = \int_{t0}^{tm} \varepsilon dt$$

where: W_ε is obtained by integrating ε over the main phase of each geomagnetic storm, from t_0 to t_m.
All units are in SI

$r(B_{avg}, Dst) = –0.66$
$r(V_{avg}, Dst) = –0.37$
$r(\rho_{avg}, Dst) = –0.25$
$r(T_{avg}, Dst) = –0.23$
$r(W_{\varepsilon}, Dst) =$ **–0.71**

$r(V, Dst)_0 = –0.20$
$r(V, Dst)_{-1} = –0.21$
$r(V, Dst)_{-2} = –0.21$
$r(V, Dst)_{-3} = –0.29$

$r(\rho, Dst)_0 =$ **–0.07**
$r(\rho, Dst)_{-1} =$ **–0.13**
$r(\rho, Dst)_{-2} =$ **0.07**
$r(\rho, Dst)_{-3} =$ **0.09**

$r(Bz, Dst)_0 = 0.1$
$r(Bz, Dst)_{-1} = 0.46$
$r(Bz, Dst)_{-2} =$ **0.76**
$r(Bz, Dst)_{-3} =$ **0.68**

$r(Bs \cdot V, Dst)_0 = –0.28$
$r(Bs \cdot V, Dst)_{-1} = –0.48$
$r(Bs \cdot V, Dst)_{-2} =$ **–0.74**
$r(Bs \cdot V, Dst)_{-3} =$ **–0.74**

$r(Tp, Dst)_0 =$ **0.16**
$r(Tp, Dst)_{-1} =$ **0.18**
$r(Tp, Dst)_{-2} =$ **0.03**
$r(Tp, Dst)_{-3} =$ **0.01**

Superposed epoch analysis

Were computed:

- IP structures parameters (B, Bz, speed, temperature, density),
- geomagnetic indices (Dst and Kp) and Akasofu coupling function;

Dst and Bz

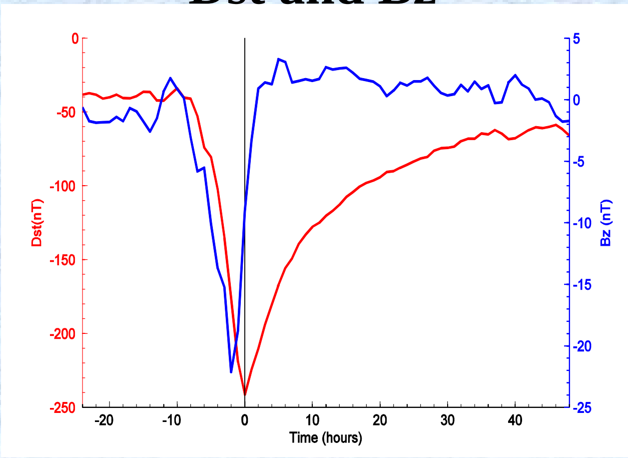

Dst and Kp

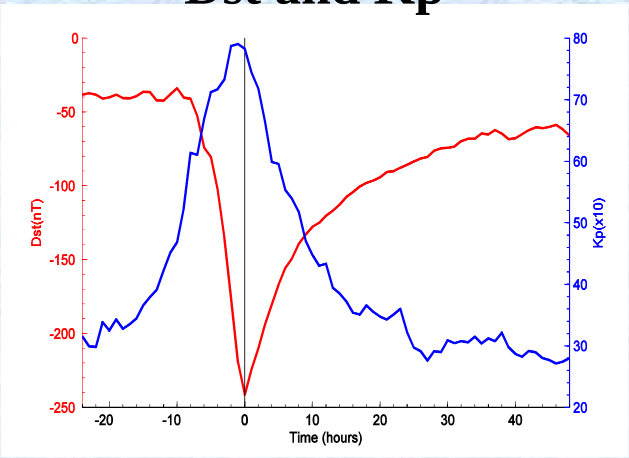

Dst and Akasofu function

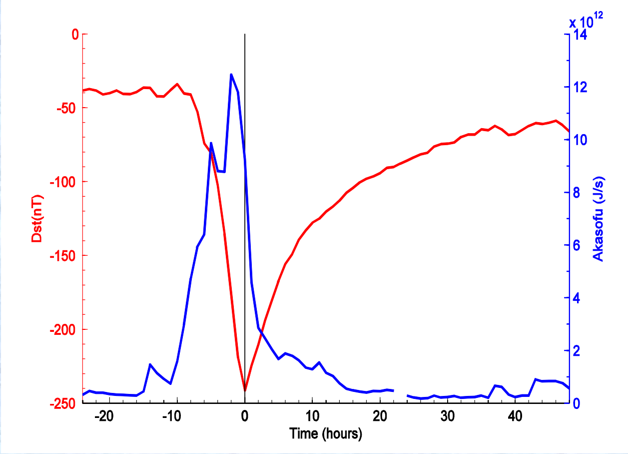

Kp and Akasofu function

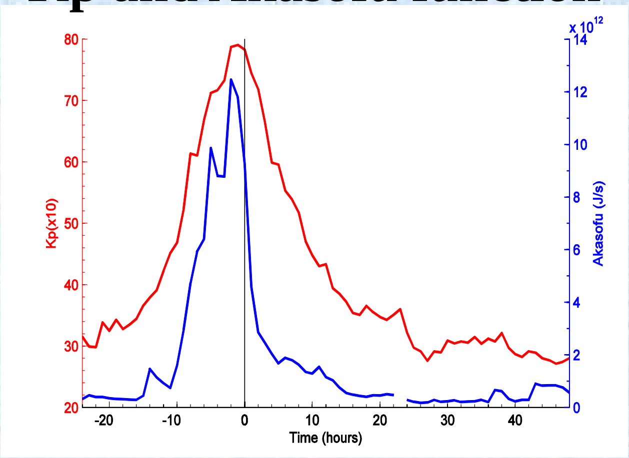

- All 25 strong geomagnetic storms, with minimum Dst ≤ –150nT meet the GT criteria, (Bs > 10 nT for long durations (t > 3 h) of time) (Echer et al. 2008).

- The superposed epoch analysis revealed the strong dependence of the geomagnetic storm intensity to the southward component of the interplanetary magnetic field, Bz, which leads to reconnection processes of the IP structures and Earth's front-side magnetic field.

- It was observed a tight dependence between the Akasofu coupling function and the Dst and Kp geomagnetic indexes. This fact reveals the importance of the reconnection processes for the amount of the energy injected into the magnetosphere in the main phase of each geomagnetic storm.

- The Kp index reaches is maximum values 1–2 hours before minimum Dst, revealing the fact that the field at higher latitudes are faster disturbed than the field around the Earth equator.

Summary

- 25 severe geomagnetic storms (Dst < -150 nT) where observed in the period 1996 – 2006 whose signatures on the Sun could be identified (57 CMEs could have produced these storms).

- The **25 ICMEs** in our study were correlated to **57 eruptive events**. All these 57 CMEs were **halo CMEs** (partial or full), directed towards Earth, and the majority emerged from **complex active regions** (βγ or βγδ magnetic configuration).

- The study of the flare - CME relationship showed **no correlation** between the flare importance (Q_x) and the Dst index.

- The CME speed analysis revealed the fact that **the speed of the CME changed while propagating into the interplanetary space** due to its interaction with the ambient solar wind or/and the interaction with other CMEs.

- Almost all storms (96%) occurred in the maximum (16 storms, 64%) and the declining phases (8 storms, 32%) of SC23.

- The most geoeffective IP structures during the 23rd SC were: sMC, Sh+MC and Sh.

- Bz and Bs·V parameters measured 2-3 hours earlier than Dst_{min} vs. Dst_{min} had the biggest correlation.

- The strong dependence of geomagnetic indices Dst and Kp to the Bz component of the interplanetary magnetic field and to the Akasofu coupling function reveals the significant role played by the reconnection processes to the amount of the energy injected into the magnetosphere in the main phase of each geomagnetic storm.

- The Kp index has its maximum value at about one to two hours before the minimum Dst, showing that the field at higher latitudes are faster disturbed than the field around the Earth equator.

Thank you for your attention!